


Morphological and functional assessment of the uterus: “one-stop shop imaging” using a compressed-sensing accelerated, free-breathing T1-VIBE sequence

Acta Radiologica
2021, Vol. 62(5) 695–704
© The Foundation Acta Radiologica
2020
Article reuse guidelines:
sagepub.com/journals-permissions
DOI: 10.1177/0284185120936260
journals.sagepub.com/home/acr


Daniel Hausmann^{1,2} , Diana Kreul³, Markus Klarhöfer³,
Dominik Nickel⁴, Robert Grimm⁴, Berthold Kiefer⁴ ,
Philipp Riffel², Ulrike I Attenberger⁵, Frank G Zöllner⁶ and
Rahel A Kubik-Huch¹ 

Abstract

Background: The combination of motion-insensitive, high-temporal, and spatial resolution imaging with evaluation of quantitative perfusion has the potential to increase the diagnostic capabilities of magnetic resonance imaging (MRI) in the female pelvis.

Purpose: To compare a free-breathing compressed-sensing VIBE (fbVIBE) with flexible temporal resolution (range = 4.6–13.8 s) with breath-hold VIBE (bhVIBE) and to evaluate the potential value of quantifying uterine perfusion.

Material and Methods: A total of 70 datasets from 60 patients (bhVIBE: n = 30; fbVIBE: n = 40) were evaluated by two radiologists. Only temporally resolved reconstruction (fbVIBE) was performed on 30 of the fbVIBE datasets. For a subset (n = 10) of the fbVIBE acquisitions, a time- and motion-resolved reconstruction (mrVIBE) was evaluated. Image quality (IQ), artifacts, diagnostic confidence (DC), and delineation of uterine structures (DoS) were graded on Likert scales (IQ/DC/DoS: 1 (non-diagnostic) to 5 (perfect); artifacts: 1 (no artifacts) to 5 (severe artifacts)). A Tofts model was applied for perfusion analysis. Ktrans was obtained in the myometrium (Mm), junctional zone (Jz), and cervix (Cx).

Results: The median IQ/DoS/DC scores of fbVIBE (4/5/5; $\kappa > 0.7$ –0.9) and bhVIBE (4/4/4; $\kappa = 0.5$ –0.7; $P > 0.05$) were high, but Artifacts were graded low (fbVIBE/bhVIBE: 2/2; $\kappa = 0.6/0.5$; $P > 0.05$). Artifacts were only slightly improved by the additional motion-resolved reconstruction (fbVIBE/mrVIBE: 2/1.5; $P = 0.08$); fbVIBE was preferred in most cases (7/10). Significant differences of Ktrans values were found between Cx, Jz, and Mm (0.12/0.21/0.19; $P < 0.05$).

Conclusion: The fbVIBE sequence allows functional and morphological assessment of the uterus at comparable IQ to bhVIBE.

Keywords

Magnetic resonance imaging, female, cervix uteri, uterus, artifacts, magnetic resonance perfusion

Date received: 9 April 2020; accepted: 17 May 2020

Introduction

Functional analysis of pelvic diseases has become significantly more important in recent years. Contrast-enhanced magnetic resonance imaging (MRI) is now an integral part of most uterus examinations.

In its current guidelines, the European Society of Urogenital Radiology (ESUR) recommends dynamic contrast-enhanced (DCE) MRI for the staging of endometrial carcinomas and for facilitating patient selection before fertility-sparing management in organ-confined

¹Department of Radiology, Kantonsspital Baden, Baden, Switzerland

²Department of Clinical Radiology and Nuclear Medicine, University Medical Center Mannheim, Medical Faculty Mannheim, Heidelberg University, Mannheim, Germany

³Siemens Healthcare AG, Zürich, Switzerland

⁴MR Applications Predevelopment, Siemens Healthcare GmbH, Erlangen, Germany

⁵Department of Radiology, University Hospital Bonn, Bonn, Germany

⁶Computer Assisted Clinical Medicine, Mannheim Institute for Intelligent Systems in Medicine, Medical Faculty Mannheim, Heidelberg University, Mannheim, Germany

Corresponding author:

Daniel Hausmann, Institute of Radiology, Kantonsspital Baden, Im Ergel 1, 5404 Baden, Switzerland.

Email: Daniel.hausmann@ksb.ch

endometrial carcinoma and early stage cervical carcinoma that qualifies for trachelectomy (1,2). Numerous studies have shown that multiphase contrast-enhanced MRI has high diagnostic accuracy for detecting deep myometrial invasion (MI) of endometrial carcinoma, an important prognostic factor that potentially influences not only treatment decisions, but also prognosis (3–5). Moreover, infiltrations of the bladder and rectal wall in advanced tumor stages can be seen better on contrast-enhanced sequences than on non-contrast-enhanced acquisitions (6).

Besides, functional applications of DCE based on quantitative perfusion evaluation have gained importance. DCE allows for the assessment of vascular permeability and blood flow using various kinetic models (7). Of these, the two-compartment Tofts model with calculation of K_{trans} values is the most established (8). In this context, K_{trans} is a marker for capillary leakage (e.g. in fragile tumor vessels) (9).

Ippolito et al. (10) published a study suggesting that DCE can generate important quantitative information for the detection and grading of endometrial carcinomas. Another study of endometrial cancer showed that quantitative perfusion analysis using DCE helps to identify patients at increased risk of recurrence (11). Further work found that DCE-MRI contains valuable information about the hypoxia fraction of squamous cell carcinomas of the uterine cervix with possible implications for individualized therapy (12). Unfortunately, the standard DCE sequences are prone to patient motion artifacts, which may impair the diagnostic accuracy of the examination, and they are not fast enough for accurate perfusion quantification.

New sequences accelerated by compressed sensing (13) enable both qualitative and quantitative assessment of organs in a single acquisition (14,15) and master the tradeoff between high spatial and high temporal resolution, which is a prerequisite for perfusion quantification (16,17). Golden-angle radial sparse parallel MRI was the first highly accelerated free-breathing sequence with artifact reduction achieved by motion-insensitive radial acquisition, and it has the possibility of simultaneous perfusion quantification (18,19). A disadvantage of golden-angle radial sparse parallel MRI is the computational effort required, which in practice can only be supplied by an external reconstruction server for older MRI scanners.

In the present study, a prototypical Cartesian free-breathing compressive sensing (CS) VIBE (fbVIBE) was applied, which allows reconstructions with variable temporal resolution suitable for quantitative perfusion analysis with clinically acceptable reconstruction times on conventional scanner hardware. The application addresses motion through the acquisition of a

navigation signal that is used for gating or motion state-resolved reconstruction.

The aim of the present study was to compare the image quality of this new sequence with the clinically established breath-hold VIBE (bhVIBE) and to explore the benefits of additional quantitative perfusion analysis. Finally, the potential dependence of perfusion in different regions of the uterus on the menstrual cycle is evaluated.

Material and Methods

Ethics statement

The present study was approved by the Ethics Committee of northwestern and central Switzerland (2018-01586). The requirement of individual written informed consent was waived.

Patient selection

From August 2018 to March 2019, 30 consecutive female patients referred for MRI of the uterus for various reasons were examined using fbVIBE (mean age = 42 ± 15 years). A bhVIBE collective (mean age = 49 ± 20 years) of the same size was assembled randomly from our MRI archive. In these 60 patients, subjective image perception was compared between both sequences.

Quantitative perfusion analysis could only be performed in the fbVIBE collective because of the high spatiotemporal resolution provided by the VIBE sequence with CS reconstruction. Calculation of the perfusion maps was not possible in four patients because of a software error, resulting in a total group size of 26 patients for perfusion measurements.

In 10 patients from the fbVIBE collective, an additional motion-resolved reconstruction to reduce motion artifacts was performed and artifacts were compared with the time-resolved-only approach.

MRI acquisition

Patients fasted for 4 h before the exam and were prepared with glucagon as a standard to reduce artifacts due to bowel movement (20).

MR images were acquired using 1.5-T MR scanners (MAGNETOM Aera/Avanto Fit, Erlangen, Germany) equipped with 50-channel coil setups (18-channel body coil and 32-channel spine coil). Patients were placed into the MRI scanner in a head-first supine position. The prototypical T1-weighted (T1W) gradient-echo sequence after injection of gadopentetate dimeglumine (Dotarem[®], Guerbet, Paris, France) was performed in free-breathing for subsequent compressed-sensing reconstruction. For contrast-enhanced imaging,

0.1 mmol/kg Dotarem was administered at a rate of 2 mL/s. Contrast application was started 5 s after the sequence was initiated. The temporal resolution was <5 s for accurate perfusion estimation in the early phase and was then gradually increased to about 14 s for improved morphologic imaging. Total DCE acquisition time was 2 min 24 s. Protocol parameters are detailed in Table 1.

Image reconstruction

In addition to time-resolved compressed-sensing reconstruction of CS VIBE (fbVIBE), motion-resolved reconstruction was investigated.

The time-resolved compressed-sensing reconstruction used for fbVIBE is an iterative optimization of a cost function that consists of a data fidelity term and a sparsity-enforcing regularization term. Coil sensitivity maps obtained by a separate calibration scan were used for the data fidelity term. The regularization was the L1-norm of a multidimensional Haar transformation with different regularization weights for different levels. Images were reconstructed online during acquisition on the scanner-integrated CPU with a duration of approximately 8 min.

The sequence's acquisition of additional projections interleaved with the imaging acquisition allows for the additional extraction of a navigation signal along the head-foot axis. The insertion of these additional navigation scans has no practical effect on the acquisition time and allows retrospective reconstructions of the dataset that relies on the navigation signal.

For randomly selected cases ($n=10$), a motion-resolved reconstruction (mrVIBE) was performed to evaluate the importance and effects of motion compensation in the reconstruction. The mrVIBE reconstruction extracts a one-dimensional navigation signal from the navigation scans and assigns the acquired image data to several motion states (six in this work). These motion states are considered an additional dimension in the reconstruction, with regularization enforcing similarity between the neighboring motion states.

Therefore, the number of reconstructed image volumes is multiplied by the number of designated motion states, as is the reconstruction duration. In the clinical setting, MR reconstruction can be achieved in approximately 10 min on GPU-equipped scanners only. The raw data were hence exported and reconstructed offline.

Image quality assessment

Two radiologists (Observer 1 and Observer 2, with 24 and 9 years of pelvic imaging experience, respectively) who were unaware of the patients' clinical data independently evaluated all images, including both fbVIBE and bhVIBE. Both readers assessed the images separately. Image quality (IQ), the quality of the BLADE/Ktrans fusion map (IQKtrans), artifacts, delineation of structures (DoS), and diagnostic confidence (DC) were rated on Likert-type scales (IQ/IQKtrans/DoS/DC: 1 = non-diagnostic to 5 = perfect; artifacts: 1 = no artifacts to 5 = severe artifacts). Images were assessed on a Centricity PACS workstation (Radiology RA 1000, GE Healthcare, USA).

Pharmacokinetic analysis

Perfusion quantification of the reconstructions was done using a commercially available workstation (*syngo.via* Tissue4D, version VB30; Siemens Healthcare, Erlangen, Germany). After elastic motion correction of the dynamic series, the Tofts model was applied using a population-based arterial input function (21). In this initial investigation, a constant T1 relaxation time of 2000 ms was assumed for the entire uterus, which is slightly higher than the values published in recent literature (22). The results should therefore be regarded as an explorative, semi-quantitative approach that should allow us to demonstrate the feasibility and potential of pharmacokinetic modeling.

For measurement of Ktrans, ROIs of similar size were carefully placed on the cervix (Cx), junctional zone (Jz), and myometrium (mm) on the fbVIBE/Ktrans fusion map (Fig. 1).

Table 1. Imaging Protocol.

	Slice thickness (mm)	FOV (mm)	TR (ms)	TE (ms)	FA (°)	Temporal resolution (s)
fbVIBE	2.5	260	4.75	1.83	12	4.6–13.8 (19 acquisitions) (1–12: 4.6; 13–14: 9.2; 15–19: 13.8)
bhVIBE	2.5	260	7.03	2.39	12	18

Except for the temporal resolution, the most relevant protocol parameters are similar between both sequences. bhVIBE, breath-hold VIBE; FA, flip angle; fbVIBE, free-breathing VIBE; FOV, field of view; TE, echo time; TR, repetition time.

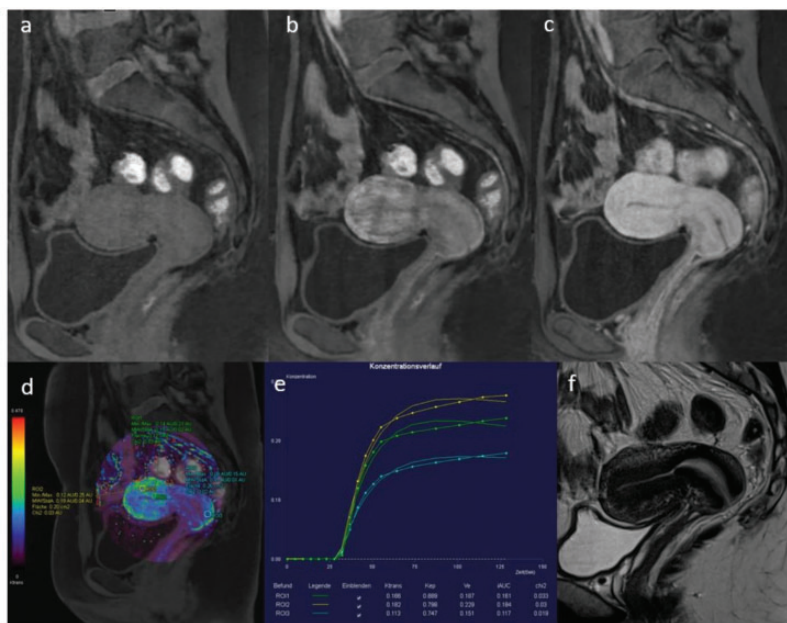


Fig. 1. The high temporal resolution of fbVIBE (a–c) was used to generate color-coded Ktrans maps (d). Ktrans was measured in the cervix, junctional zone, and myometrium. Enhancement curves were also generated (e). The uterocervical angle of fbVIBE is increased compared with that of T2 BLADE (f) due to the bladder filling during the course of the examination, which can cause a mismatch between morphological images and the perfusion map.

Statistical analyses

SPSS (Version 22; IBM SPSS Statistics, Armonk, NY, USA) was used for statistical evaluation. Mann–Whitney U tests were applied for assessment of subjective image perception (IQ, IQKtrans, DoS, artifacts, and DC) to compare fbVIBE with bhVIBE. For the assessment of all image quality parameters, only the ratings of the senior observer were used. The Bonferroni-corrected Welch-ANOVA test was used to compare Ktrans between all three regions (Cx, Jz, and Mm). Finally, the readers' agreement in their evaluations of image quality criteria was assessed by Cohen's Kappa. Boxplots were applied for comparisons of Ktrans and image quality parameters.

Results

Image quality and artifacts

No significant differences regarding the comparisons of IQ/DoS/DC and artifacts between fbVIBE with time-resolved reconstruction and bhVIBE were observed (Table 2; Figs. 2–5). IQKtrans received relatively good ratings (median = 4 by both readers), despite a heterogeneous and blurry appearance of the color-coded Ktrans maps in some cases and mismatches between morphology and Ktrans on the T2 BLADE/Ktrans fused images (Fig. 1). The agreement between

the observers was good ($K > 0.5$) for fbVIBE and bhVIBE regarding all subjective comparisons (Table 2).

Motion-resolved reconstruction

The importance of motion-resolved reconstruction for DCE of the pelvis was explored on a subset of the acquisitions. Artifacts were only slightly improved by MR reconstruction, and the difference was not significant (fb/mrVIBE = 2/1.5; $P = 0.08$). In some cases, the edges of organ borders were somewhat sharper, but the lower lesion contrast was considered to be disadvantageous (Fig. 6). Therefore, fbVIBE was preferred over mrVIBE in most cases (7/10).

Perfusion quantification

Significant differences in Ktrans values between Cx, Jz, and Mm were found (0.12, 0.21, 0.19, respectively; $P < 0.05$; Fig. 7). However, no significant difference was observed between the Ktrans values in Jz and Mm.

Discussion

The fbVIBE sequence allows robust morphological assessment of the phases of the uterus at high image quality and high temporal resolution. In our collective, we observed satisfactory assessment of the zonal anatomy of the uterus with good distinctness between the internal and external myometrium (DoS: 5; Fig. 2)

Table 2. IQ parameters.

	fbVIBE (n = 30)	bhVIBE (n = 30)	K (fb)	K (bh)
IQ	4	4	0.89	0.53
DoS	5	4	0.71	0.64
DC	5	4	0.81	0.70
Artifacts	2	2	0.59	0.54
P	>0.05		NA	NA

Slight, insignificant advantages of fbVIBE regarding IQ parameters were found. The agreement between the radiologists was basically good, with some exceptions (IQ/artifacts).

bhVIBE, breath-hold VIBE; DC, diagnostic confidence; DoS, delineation of structures; fbVIBE, free-breathing VIBE; FOV, field of view; IQ, image quality; NA, not applicable.

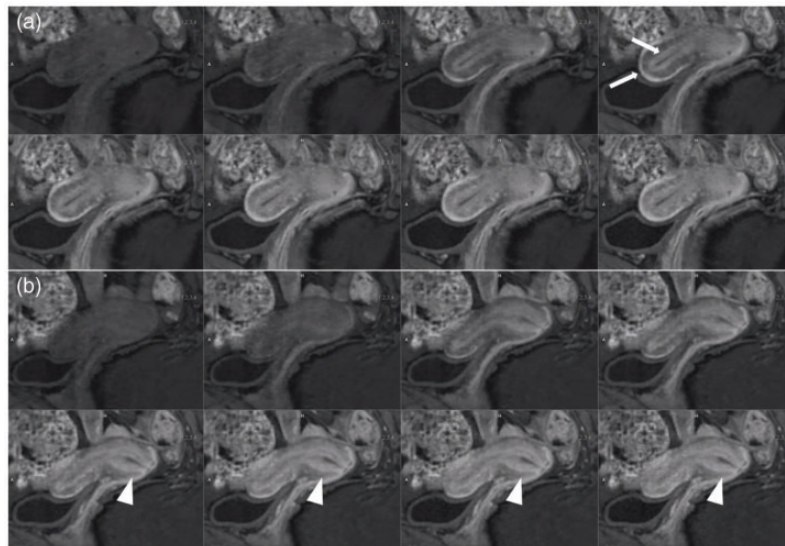


Fig. 2. Multiphasic morphological assessment of the uterus allows for accurate differentiation of its different zones. The organ boundaries are sharply delineated and the junctional zone can be clearly separated from the myometrium (a; arrows). The cervix can also be assessed well in different contrast agent phases (b; arrowhead).

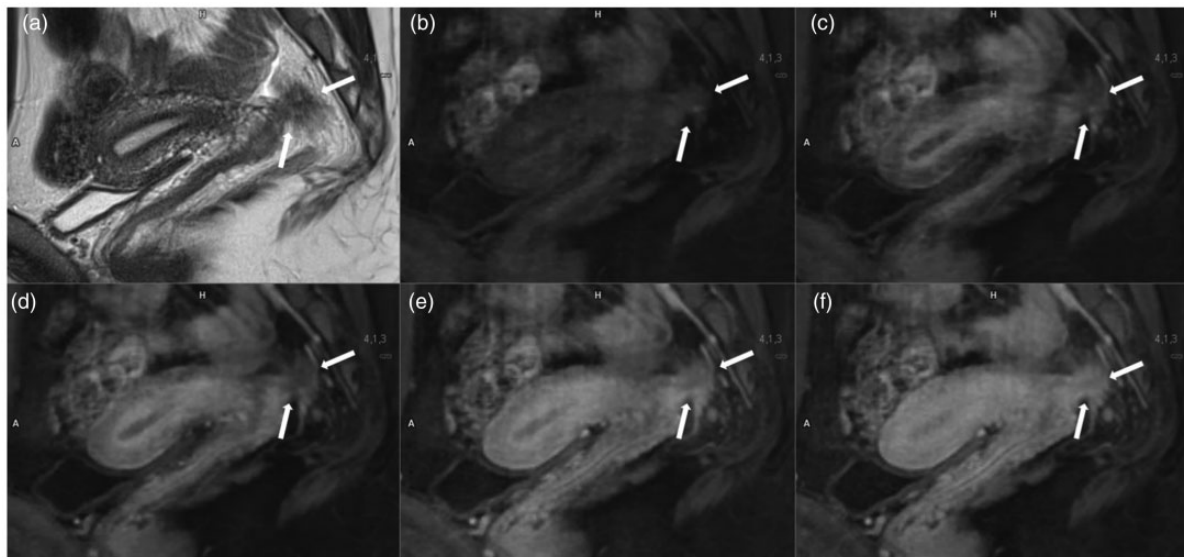


Fig. 3. Images of a 28-year-old patient with deep infiltrating endometriosis, which appears hypointense in the T2 BLADE sagittal (a). The high temporal resolution is particularly useful for evaluating the depth infiltration of endometriosis into adjacent structures such as the anterior rectal wall (b–f), with considerable implications for surgical planning.

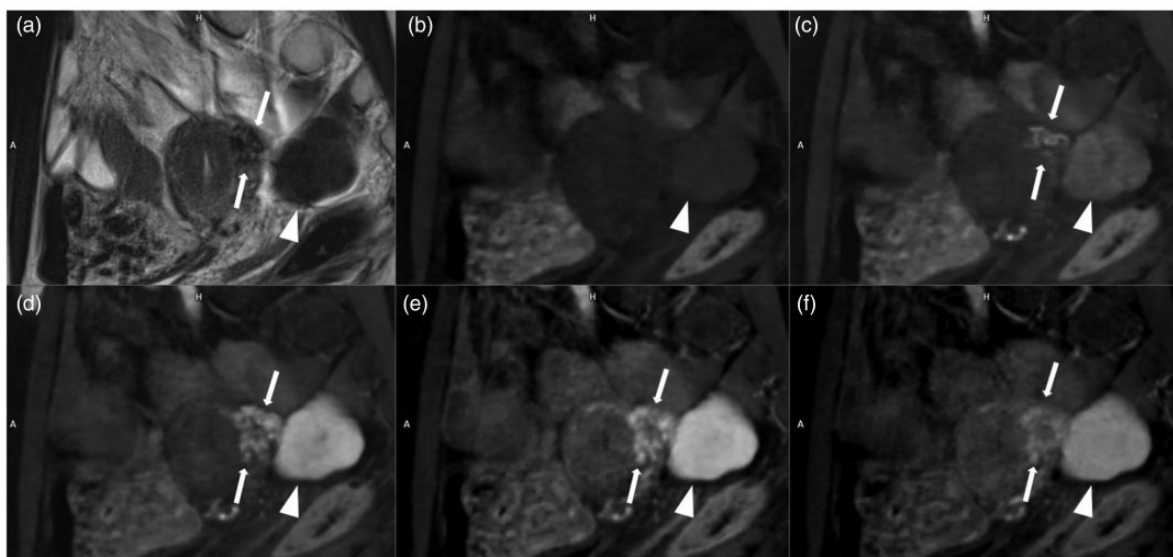


Fig. 4. Images of a 37-year-old patient with multiple leiomyomas. The uterine origin of a pedunculated leiomyoma (arrowhead) is clearly demonstrated by the “vascular pedicle sign,” which is the connection of the vessels from the myometrium via a style to the leiomyoma (arrows).

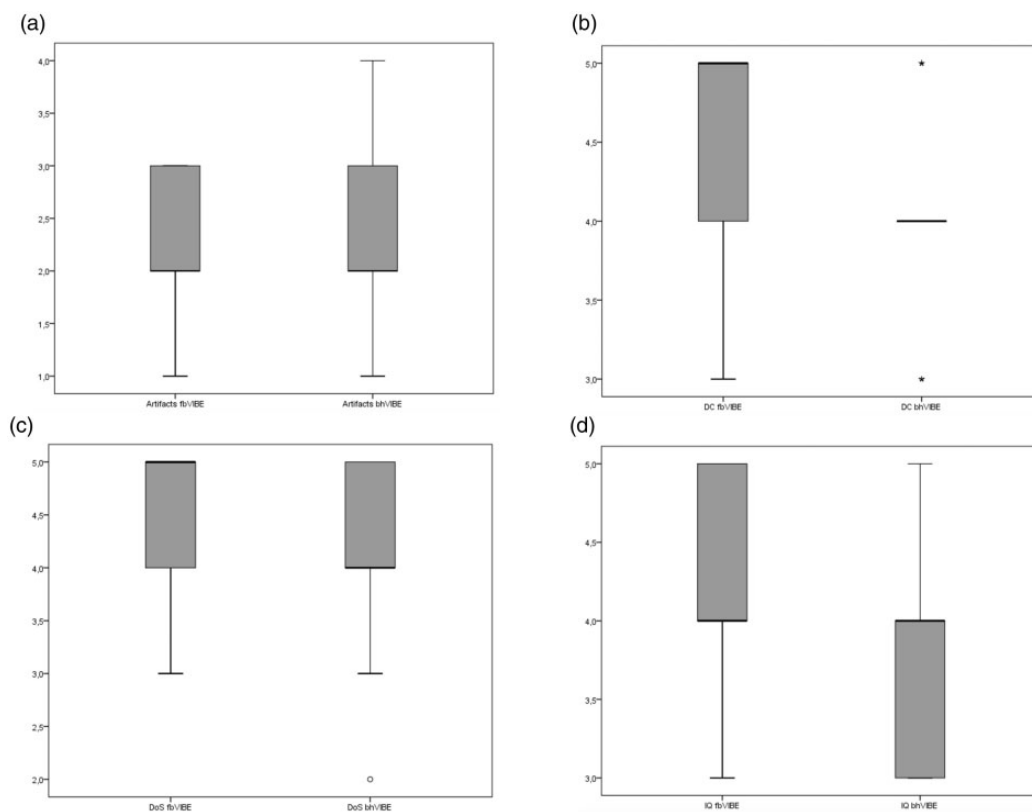


Fig. 5. No significant differences of IQ/DoS/DC or artifacts between fbVIBE and bhVIBE were observed. However, DoS and DC of fbVIBE were rated slightly higher than bhVIBE (median: 5 (fbVIBE) vs. 4 (bhVIBE)), probably owing to the multiphase visualization of the uterus, which enabled detailed assessment of the zonal anatomy and artifact reduction by CS reconstruction. CS, compressive sensing; DC, diagnostic confidence; DoS, delineation of structures; IQ, image quality.

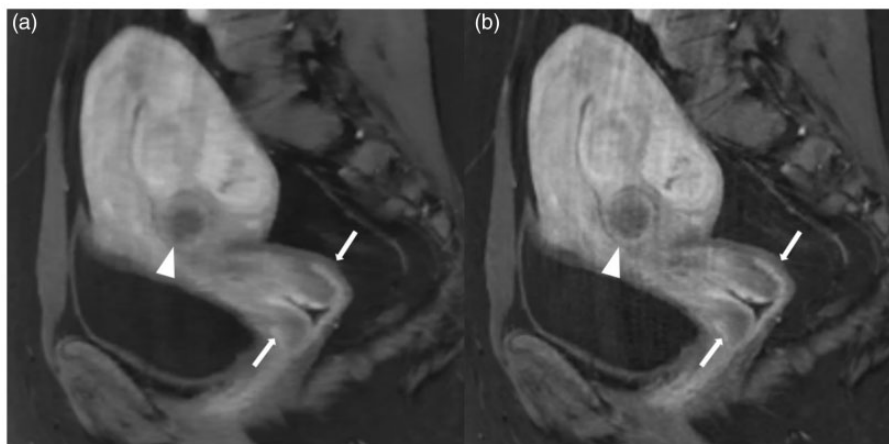


Fig. 6. In many cases, motion-state-resolved reconstruction (a) leads to a reduction of vertical motion artifacts along the abdominal wall. However, the contrast of lesions (leiomyoma (arrowhead)) or structures (cervix (arrows)) is often decreased compared with that in time-resolved only reconstruction (a versus b).

upon motion-insensitive spatiotemporal reconstruction of the free-breathing acquisition and multiphase visualization of the uterus.

Contrast-enhanced MRI can be useful for assessing the uterus for a variety of reasons. First, non-contrast-enhanced morphological imaging may have a variety of pitfalls, particularly in postmenopausal women. Loss of definition of Jz often occurs. Additionally, myometrial compression by polypoid tumors, a poor tumor-to-myometrium contrast, leiomyomas, and adenomyosis may limit the interpretability of the images (23).

DCE could also contribute to the staging and response assessment for cervical cancer (24). Adding fast DCE improves the accuracy of staging to 91% and helps to detect rectal or bladder infiltration (25). Contrast-enhanced sequences can also assist with differentiating residual tumors and radiation fibrosis (26).

DCE is controversial for the staging of endometrial cancer. A meta-analysis has shown that DCE-MRI has similar sensitivity to T2-weighted (T2W) imaging but is more specific for the detection of deep infiltration of the myometrium (MI) (3).

A meta-analysis by Andreano et al. (27) found that DWI and DCE had 88% and 94% accuracy, respectively. A recent larger meta-analysis also suggested similar peer performance of DCE and DWI for recognition of MI (28). The later contrast medium phases provide the best conditions for identification of MI, so DCE would not be absolutely necessary here.

In rare cases, in patients of childbearing age, it can be important to maintain reproductive capacity, which may be possible in endometrium-confined grade-1 endometrioid adenocarcinomas and premalignant diseases. In this context, the ESUR recommends DCE to assess the presence of intact subendometrial enhancement (1). Uninterrupted enhancement of the

subendometrial zone has been observed to be best at approximately 35–40 s after contrast administration and requires very accurate timing to implement conventional DCE sequences (5). The high temporal resolution of fbVIBE could be beneficial for identification of such early stages of endometrial carcinoma and may enable more individualized treatment.

Image quality in the upper abdomen could be further improved by applying motion-resolved reconstruction (29–31). In the pelvis, where motion artifacts play a comparatively minor role, no significant improvement in image quality has been shown. Motion-resolved reconstructions had lower contrast compared with reconstructions that were only temporally resolved, and the contours of lesions or the borders of organ regions could not be clearly distinguished, which could interfere with the detectability of small lesions or the assessment of the infiltration depths of malignant tumors or endometriosis. Hence, time-resolved reconstruction was preferred in most cases. We speculate that the one-dimensional navigation signal is not well suited to describe the superposition of breathing motion and peristalsis in the pelvis. In contrast to the upper abdomen, for which most scans are attributed to the exhaled motion state, we also observed that the pelvic scans are assigned more uniformly over the motion states. This results in a higher effective acceleration for each reconstructed volume, which may explain the lower contrast and smoother image impressions.

The advantages of three-dimensional (3D) DCE over two-dimensional T2W imaging include allowing thinner slices, higher spatial resolution, and additional perfusion information, potentially enabling multiple future applications.

A study by Haldorsen et al. (11) observed that aggressive subtypes of endometrial carcinomas show

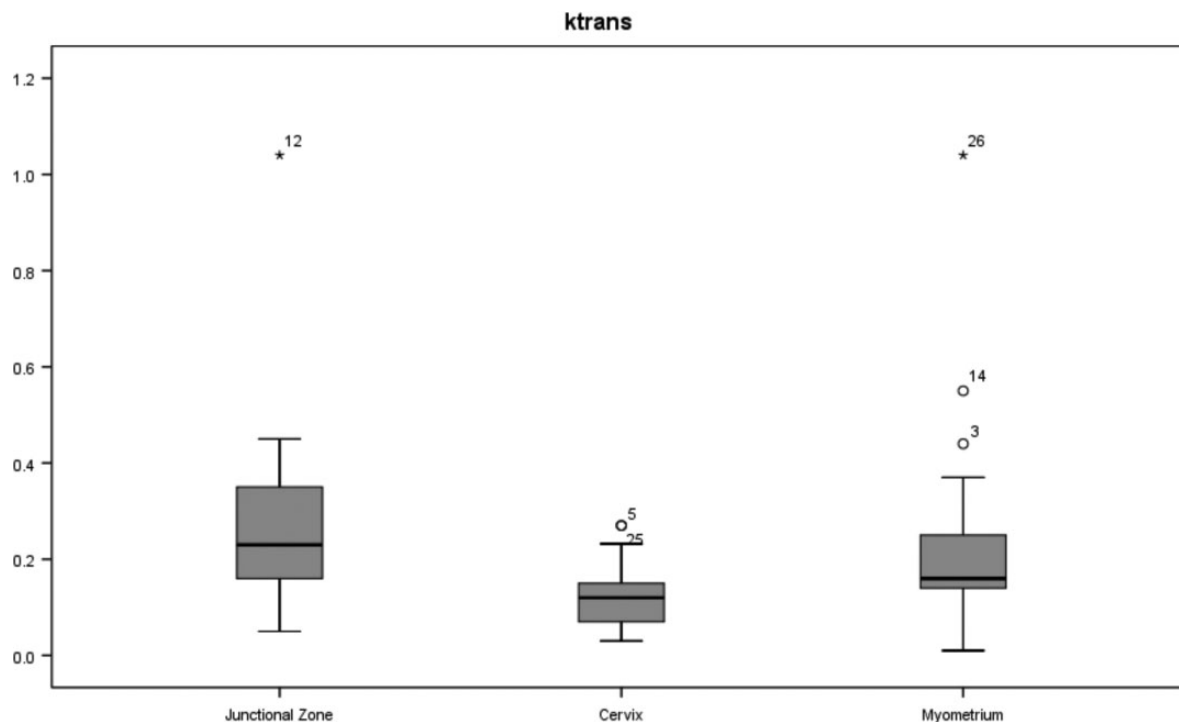


Fig. 7. Ktrans in the different zones of the uterus. Jz, junctional zone; Mm, myometrium; Cx, cervix.

less tumor perfusion than less aggressive tumors do. Increased tumor transit time and decreased blood flow were associated with poorer survival. Thus, DCE could be suitable as a biomarker for preoperative risk stratification. Another recent study indicated that low tumor blood flow and a low rate constant for contrast agent intravasation (k_{ep}) were associated with a high-risk histological subtype (32).

In four patient-derived xenografts, Hauge et al. (12) found an inverse correlation between Ktrans and the hypoxic tumor fraction. That finding is of particular importance for individualized therapy planning with antiangiogenic substances.

There may be other interesting applications of quantitative perfusion analysis outside of tumor diagnostics e.g. in deep infiltrating endometriosis (Fig. 3). In this context, uterine leiomyoma is a common disease that affects approximately 25% of women, and it is associated with pain, dyspareunia, pollakiuria, and infertility.

MRI could be a tool not only to detect uterine leiomyomas but also to predict the outcome of embolization (33). Interventionalists could use 3D-reconstructed MR angiography to evaluate pelvic vessels before intervention, reduce fluoroscopy time, and consecutively reduce periprocedural radiation and the contrast agent dose (34–36). Sadick et al. (37) showed in seven patients that the therapeutic success of uterine artery embolization can be monitored with perfusion quantification.

The “one-stop” approach of fbVIBE could help to plan interventions by recognizing the feeding vessels of leiomyomas owing to its high spatiotemporal resolution (Fig. 4). The method could also help with response assessment by means of perfusion quantification.

In the present study, the image quality of the fusion of color-coded parametric Ktrans maps and sagittal T2 BLADE images was good ($IQK_{trans} = 4$; Fig. 1), and the Ktrans values in Jz, Cx, and Mm could be determined (Fig. 7). In some cases, the image quality was rated as insufficient, which could be explained by inadequate patient preparation, resulting in factors including a moderately filled bladder that could affect the angle of uterine anteversion.

The present study has some limitations. First, for the conversion of signal intensities to concentration time curves, we used a fixed T1 value rather than performing T1 mapping. Owing to the low injected dose of contrast agent, a linear relationship between contrast agent concentration and signal intensity was assumed. Second, the results of the quantitative Ktrans evaluation should be judged carefully because of the small size of the collective. Finally, patients were assigned to the protocol via routine clinical referrals and selected solely based on receiving the MR protocol for uterine pathologies. The patient population is therefore heterogeneous, with various benign and malignant uterine pathologies, but also normal findings. Theoretically,

the combination of high morphological and temporal resolution should prove beneficial, but the results do not allow us to draw any conclusions regarding improvement of diagnostic confidence for different uterine pathologies.

In conclusion, fbVIBE allows for morphological and functional assessment of the uterus in a single acquisition with good overall image quality, which may be useful for characterizing lesions or tumor staging. Perfusion analysis and robust high temporal resolution imaging may be beneficial for evaluation of various uterine diseases. Interesting future applications of multiphase DCE with perfusion quantification could include treatment planning before and response assessment after embolization of leiomyomas (Fig. 4) or evaluation of bladder or intestinal wall infiltration by endometriosis (Fig. 3). Further studies are intended that will combine T1 mapping with fbVIBE to explore the benefits of “full” perfusion quantification in selected collectives and pathologies.

Acknowledgements

The authors thank Richard Lipkin, Edanz Group (www.edanzediting.com/ac), for editing a draft of this manuscript.

Declaration of conflicting interests

The author(s) declare no potential competing interest with respect to the research, authorship, and/or publication of this article.

Funding

The author(s) received no financial support for the research, authorship, and/or publication of this article.

ORCID iDs

Daniel Hausmann  <https://orcid.org/0000-0002-3816-3302>
 Berthold Kiefer  <https://orcid.org/0000-0003-1406-8033>
 Rahel A Kubik-Huch  <https://orcid.org/0000-0002-3636-8697>

References

1. Nougaret S, Horta M, Sala E, et al. Endometrial cancer MRI staging: updated guidelines of the European Society of Urogenital Radiology. *Eur Radiol* 2019;29:792–805.
2. Akita A, Shimoto H, Hayashi S, et al. Comparison of T2-weighted and contrast-enhanced T1-weighted MR imaging at 1.5 T for assessing the local extent of cervical carcinoma. *Eur Radiol* 2011;21:1850–1857.
3. Wu LM, Xu JR, Gu HY, et al. Predictive value of T2-weighted imaging and contrast-enhanced MR imaging in assessing myometrial invasion in endometrial cancer: a pooled analysis of prospective studies. *Eur Radiol* 2013;23:435–449.
4. Park SB, Moon MH, Sung CK, et al. Dynamic contrast-enhanced MR imaging of endometrial cancer: optimizing the imaging delay for tumour-myometrium contrast. *Eur Radiol* 2014;24:2795–2799.
5. Fujii S, Kido A, Baba T, et al. Subendometrial enhancement and peritumoral enhancement for assessing endometrial cancer on dynamic contrast enhanced MR imaging. *Eur J Radiol* 2015;84:581–589.
6. Balleyguier C, Sala E, Da Cunha T, et al. Staging of uterine cervical cancer with MRI: guidelines of the European Society of Urogenital Radiology. *Eur Radiol* 2011;21:1102–1110.
7. Koh TS, Bisdas S, Koh DM, et al. Fundamentals of tracer kinetics for dynamic contrast-enhanced MRI. *J Magn Reson Imaging* 2011;34:1262–1276.
8. Tofts PS, Brix G, Buckley DL, et al. Estimating kinetic parameters from dynamic contrast-enhanced T(1)-weighted MRI of a diffusable tracer: standardized quantities and symbols. *J Magn Reson Imaging* 1999;10:223–232.
9. Zollner FG, Gaa T, Zimmer F, et al. [Quantitative perfusion imaging in magnetic resonance imaging]. *Radiologe* 2016;56:113–123.
10. Ippolito D, Minutolo O, Cadonici A, et al. Endometrial cancer: diagnostic value of quantitative measurements of microvascular changes with DCE-MR imaging. *MAGMA* 2014;27:531–538.
11. Haldorsen IS, Gruner R, Husby JA, et al. Dynamic contrast-enhanced MRI in endometrial carcinoma identifies patients at increased risk of recurrence. *Eur Radiol* 2013;23:2916–2925.
12. Hauge A, Wegner CS, Gaustad JV, et al. DCE-MRI of patient-derived xenograft models of uterine cervix carcinoma: associations with parameters of the tumor microenvironment. *J Transl Med* 2017;15:225.
13. Heidkamp J, Hoogenboom M, Kovacs IE, et al. Ex vivo MRI evaluation of prostate cancer: localization and margin status prediction of prostate cancer in fresh radical prostatectomy specimens. *J Magn Reson Imaging* 2018;47:439–448.
14. Attenberger UI, Liu J, Riffel P, et al. Quantitative perfusion analysis of the rectum using golden-angle radial sparse parallel magnetic resonance imaging: initial experience and comparison to time-resolved angiography with interleaved stochastic trajectories. *Invest Radiol* 2017;52:715–724.
15. Riffel P, Zoellner FG, Budjan J, et al. “One-stop shop”: free-breathing dynamic contrast-enhanced magnetic resonance imaging of the kidney using iterative reconstruction and continuous golden-angle radial sampling. *Invest Radiol* 2016;51:714–719.
16. Othman AE, Falkner F, Weiss J, et al. Effect of temporal resolution on diagnostic performance of dynamic contrast-enhanced magnetic resonance imaging of the prostate. *Invest Radiol* 2016;51:290–296.
17. Michaely HJ, Sourbron SP, Buettner C, et al. Temporal constraints in renal perfusion imaging with a 2-compartment model. *Invest Radiol* 2008;43:120–128.
18. Feng L, Axel L, Chandarana H, et al. XD-GRASP: golden-angle radial MRI with reconstruction of extra

- motion-state dimensions using compressed sensing. *Magn Reson Med* 2016;75:775–788.
19. Feng L, Grimm R, Block KT, et al. Golden-angle radial sparse parallel MRI: combination of compressed sensing, parallel imaging, and golden-angle radial sampling for fast and flexible dynamic volumetric MRI. *Magn Reson Med* 2014;72:707–717.
 20. Gutzeit A, Binkert CA, Koh DM, et al. Evaluation of the anti-peristaltic effect of glucagon and hyoscine on the small bowel: comparison of intravenous and intramuscular drug administration. *Eur Radiol* 2012;22:1186–1194.
 21. Parker GJ, Roberts C, Macdonald A, et al. Experimentally-derived functional form for a population-averaged high-temporal-resolution arterial input function for dynamic contrast-enhanced MRI. *Magn Reson Med* 2006;56:993–1000.
 22. Takatsu Y, Okada T, Miyati T, et al. Magnetic resonance imaging relaxation times of female reproductive organs. *Acta Radiol* 2015;56:997–1001.
 23. Sala E, Rockall A, Kubik-Huch RA. Advances in magnetic resonance imaging of endometrial cancer. *Eur Radiol* 2011;21:468–473.
 24. Balleyguier C, Sala E, Da Cunha T, et al. Staging of uterine cervical cancer with MRI: guidelines of the European Society of Urogenital Radiology. *Eur Radiol* 2011;21:1102–1110.
 25. Van Vierzen PB, Massuger LF, Ruys SH, et al. Fast dynamic contrast enhanced MR imaging of cervical carcinoma. *Clin Radiol* 1998;53:183–192.
 26. Kinkel K, Ariche M, Tardivon AA, et al. Differentiation between recurrent tumor and benign conditions after treatment of gynecologic pelvic carcinoma: value of dynamic contrast-enhanced subtraction MR imaging. *Radiology* 1997;204:55–63.
 27. Andreano A, Rechichi G, Rebora P, et al. MR diffusion imaging for preoperative staging of myometrial invasion in patients with endometrial cancer: a systematic review and meta-analysis. *Eur Radiol* 2014;24:1327–1338.
 28. Deng L, Wang QP, Chen X, et al. The combination of diffusion- and T2-weighted imaging in predicting deep myometrial invasion of endometrial cancer: a systematic review and meta-analysis. *J Comput Assist Tomogr* 2015;39:661–673.
 29. Kaltenbach B, Bucher AM, Wichmann JL, et al. Dynamic liver magnetic resonance imaging in free-breathing: feasibility of a cartesian T1-weighted acquisition technique with compressed sensing and additional self-navigation signal for hard-gated and motion-resolved reconstruction. *Invest Radiol* 2017;52:708–714.
 30. Weiss J, Martirosian P, Wolf S, et al. Fast abdominal contrast-enhanced imaging with high parallel-imaging factors using a 60-channel receiver coil setup: comparison with the standard coil setup. *Invest Radiol* 2018;53:602–608.
 31. Hausmann D, Niemann T, Kreul D, et al. Free-breathing dynamic contrast-enhanced imaging of the upper abdomen using a Cartesian compressed-sensing sequence with hard-gated and motion-state-resolved reconstruction. *Invest Radiol* 2019;54:728–736.
 32. Fasmer KE, Bjornerud A, Ytre-Hauge S, et al. Preoperative quantitative dynamic contrast-enhanced MRI and diffusion-weighted imaging predict aggressive disease in endometrial cancer. *Acta Radiol* 2018;59:1010–1017.
 33. Cura M, Cura A, Bugnone A. Role of magnetic resonance imaging in patient selection for uterine artery embolization. *Acta Radiol* 2006;47:1105–1114.
 34. Naguib NN, Nour-Eldin NE, Hammerstingl RM, et al. Three-dimensional reconstructed contrast-enhanced MR angiography for internal iliac artery branch visualization before uterine artery embolization. *J Vasc Interv Radiol* 2008;19:1569–1575.
 35. Naguib NN, Nour-Eldin NE, Lehnert T, et al. Uterine artery embolization: optimization with preprocedural prediction of the best tube angle obliquity by using 3D-reconstructed contrast-enhanced MR angiography. *Radiology* 2009;251:788–795.
 36. Gupta A, Grunhagen T. Live MR angiographic road-mapping for uterine artery embolization: a feasibility study. *J Vasc Interv Radiol* 2013;24:1690–1697.
 37. Sadick M, Richers J, Tuschy B, et al. Feasibility of quantitative MR-perfusion imaging to monitor treatment response after uterine artery embolization (UAE) in symptomatic uterus fibroids. *Magn Reson Imaging* 2019;59:31–38.